Inorganica Chimica Acta 477 (2018) 40–50

Contents lists available at ScienceDirect

Inorganica Chimica Acta

journal homepage: www.elsevier.com/locate/ica

Research paper

Cyclometalated ruthenium(II) carbonyl complexes containing 2-(biphenylazo)phenolate ligands: Synthesis, structure, DFT study and catalytic activity towards oxidation and transfer hydrogenation

Madhan Ramesh [a], Madhu Deepan Kumar [b], Madhavan Jaccob [b], Bruno Therrien [c], Galmari Venkatachalam [a,*]

[a] PG & Research Department of Chemistry, Government Arts College, Dharmapuri 636 705, Tamil Nadu, India
[b] Computational Chemistry Laboratory, Loyola Institute of Frontier Energy (LIFE) & Department of Chemistry, Loyola College, Nungambakkam, Chennai 600 034, Tamil Nadu, India
[c] Institute of Chemistry, University of Neuchatel, 51 Avenue de Bellevaux, CH-2000 Neuchatel, Switzerland

ARTICLE INFO

Article history:
Received 17 October 2017
Received in revised form 3 January 2018
Accepted 17 February 2018
Available online 20 February 2018

Keywords:
Ruthenium(II)
C-H activation
Crystal structure
Redox properties
Catalytic activity
DFT study

ABSTRACT

2-(Biphenylazo)phenol ligands with various functional groups at the *para*-position of the phenol moiety (R = CH_3, H_2L_1; R = OCH_3, H_2L_2; R = $(CH_3)_3C$, H_2L_3; R = Cl, H_2L_4) readily undergo, upon reaction with [RuHCl(CO)$(EPh_3)_3$] (E = P, As) in toluene, cyclometalation *via* a C—H bond activation at the *ortho*-position to afford complexes of general formula [Ru(L)(CO)$(EPh_3)_2$] (E = P, L = L_1, **1**; E = P, L = L_2, **2**; E = P, L = L_3, **3**; E = P, L = L_4, **4**; E = As, L = L_1, **5**; E = As, L = L_2, **6**; E = As, L = L_3, **7**; E = As, L = L_4, **8**). The molecular structure of five complexes has been determined by single-crystal X-ray structure analysis. In each complexes, the 2-(biphenylazo)phenol ligand is coordinated to the metal center as a di-anionic tridentate CNO-ligand with two triphenylphosphine/triphenylarsine in the axial positions along with one carbonyl group in the plane of the CNO- ligand. These new cyclometalated 2-(biphenylazo)phenolate complexes show intense absorption in the visible and ultraviolet regions and the nature of these transitions has been analyzed by TD-DFT calculations. The redox behavior of the complexes was also studied by cyclic voltammetry, revealing an irreversible reduction of the metallic center. The cyclometalated ruthenium(II) complexes were used as catalysts for oxidation and transfer hydrogenation reactions and they were found to be active catalysts.

1. Introduction

The chemistry of ruthenium metal complexes and its favorable property of *ortho*-$C_{aromatic}$-H activation have been reported over the last three decades [1,2]. Cyclometalated complexes containing CN- donors of unsymmetrical ligands have been mainly utilized as phosphorescent materials in organic light emitting devices and as chemo-sensors [3]. Ruthenium complexes have been used as catalysts precursors for variety of purposes including hydrogenation, oxidation, polymerization and carbon–carbon bond formations [4]. Oxidation of primary and secondary alcohols into their corresponding aldehydes and ketones plays a central role in organic synthesis [5]. Ishii and co-workers successfully achieved aerobic oxidation using $Ru(PPh_3)_3Cl_2$ as the catalyst in the presence of hydroquinone without diminishing chemoselectivity [6]. Several ruthenium catalytic systems have been reported with a wide range of oxidants *viz*., *tert*-butyl hydroperoxide [7], hydrogen peroxide [8], molecular oxygen [9], iodosylbenzene [10], sodium periodate [11] and *N*-methylmorpholine-*N*-oxide [12]. More recently, transition metal catalyzed transfer hydrogenation reaction using isopropanol as a hydrogen source, has become an efficient method in organic synthesis [13]. Noyori et al., [14] reported that ruthenium(II) complexes in the presence of a base and isopropanol, proved to be excellent catalysts for the transfer hydrogenation of ketones under mild conditions. In addition, the NN- and ON-donors of the ligands play an important role in catalytic reactions [15,16].

It is well known from the literature that most of the cyclometalated ruthenium(II) complexes [17] containing different types of ligand including arylazo groups have been successfully used as effective catalysts for transfer hydrogenation of ketones [18]. The highly active cyclometalated ruthenium(II) catalysts (**A** & **B**) with CNN- donor atoms (see Fig. 1) as an accelerating functionality in the ligands for transfer hydrogenation reactions have been studied [19,20]. Moreover, PPh_3 ligands are known to be π-acceptor

* Corresponding author.
E-mail address: gvchem@gmail.com (G. Venkatachalam).

https://doi.org/10.1016/j.ica.2018.02.023
0020-1693/

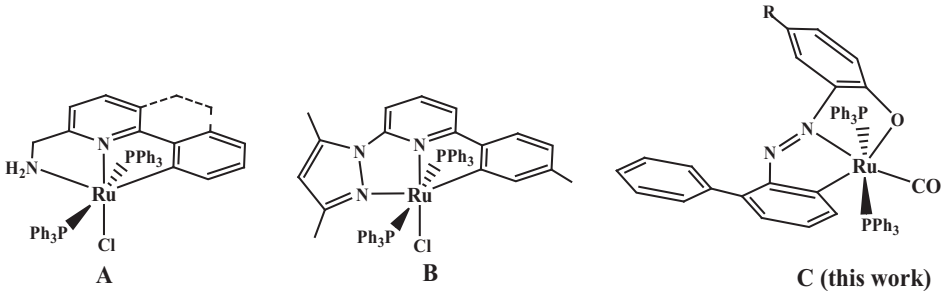

Fig. 1. Models of Ru-complexes.

ligands, which may become more labile in these complexes during a catalytic cycle. Further, the azo (N = N) group due to its strong π-acidic character stabilizes the ruthenium in lower oxidation states, while the phenolate oxygen, being a hard base, stabilizes the higher oxidation states of the metal ion [21]. Particularly, the azo function in azo-aromatics is responsible for the rich redox events in the complexes, and the design of suitable ligands containing azo functions is a natural choice for optimizations.

We herein describe the four *para*-substituted 2-(biphenylazo) phenols have been synthesized by diazotization of different *para*-substituted phenols with 2-aminobiphenyl. Then, these tridentate ligands were used to prepare a new family of cyclometalated ruthenium(II) carbonyl complexes *via* C-H activation. The interest behind the choice of this 2-(biphenylazo)phenol is that it can also act as di-anionic tridentate CNO- donor which generates five-membered metallacycles. The reaction of selected biphenylazo ligands (H_2L_1–H_2L_4) with ruthenium(II) precursors is expected to yield the corresponding cyclometalated complexes containing the chelate motif (**I**) and possible modes of coordination (**II** & **III**) Fig. 2. P. Gupta et al. [21b] reported that the reaction of [Ru$(PPh_3)_2(CO)_2(Cl)_2$] with 2-(arylazo) ligands leads to the formation of cyclometalated complexes *via* C-H activation.

In the present work, [Ru(H)Cl(CO)$(PPh_3)_3$] has been chosen as starting material to accommodate 2-(biphenylazo)phenol ligands leading to the formation of cyclometalated ruthenium complexes *via* C-H activation by the replacement of one H and one PPh_3 molecule. The [Ru(H)Cl(CO)$(PPh_3)_3$] can successfully mediate the C-H activation of 2-(biphenylazo) ligands. To the best of our knowledge, the present catalytic system is new for its oxidation and transfer hydrogenation reactions. The molecular and electronic structures of the complexes are probed with the help of X-ray crystal structure, in combination with FT-IR, electronic TD-DFT study and ^{1}H NMR spectra. The relative stabilities of oxidation and reduction states are monitored electrochemically. Further, some of the complexes have been employed as versatile catalysts for hydrogenation of ketones in the presence of *i*-PrOH/KOH and oxidation of alcohols in the presence of NMO as a more viable oxidant with moderate to high conversions.

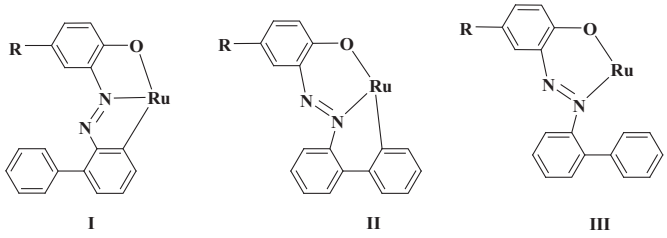

Fig. 2. Types of coordination modes for tridentate 2-(biphenylazo)phenolate ligands.

2. Results and discussion

Cyclometalated ruthenium(II) complexes of the general composition [Ru(L)(CO)$(EPh_3)_2$] (E = P, As); L = 2-(biphenylazo)phenolate ligand) were synthesized by the reaction of ruthenium precursor complexes [RuHCl(CO)$(PPh_3)_3$] and [RuHCl(CO)$(AsPh_3)_3$] with equimolar amount of the corresponding 2-(biphenylazo)phenolate ligands under reflux in toluene. The 2-(biphenylazo)phenolate ligands were observed to undergo C-H activation at one *ortho*-position of the phenyl ring in the biphenylazo fragment leading to the formation of five-membered cyclometalated rings, Scheme 1. All complexes are green in colour and found to be air stable in both the solid and liquid states at room temperature, and they are non-hygroscopic in nature. The complexes are highly soluble in common solvents such as chloroform, dichloromethane, toluene and benzene. Elemental analyses (C, H and N) were consistent with the composition proposed for all the complexes.

2.1. Mechanism of C-H activation

The proposed mechanism of C-H bond activation is depicted in Scheme 2. During the reaction of [RuHCl(CO)$(EPh_3)_3$] (E = P, As) with 2-(biphenylazo)phenolate ligands, we observed that bidentate ligands having azo and phenolate functions become tridentate, such that cyclometalated ruthenium complexes are obtained *via* orthometallation [22]. Bidentate ligands can stabilize Ru(II) or Ru (III) depending upon the nature of the donor atoms. In the first step (**I**), the hydrido and PPh_3/$AsPh_3$ ligands are replaced by O and N-donor of 2-(biphenylazo)phenolate fragment [23]. The C-H bond to be cyclometalated in the biphenyl ring is considerably weakened by the interaction of the proton with Cl-Ru bond and may be envisaged as an activated bond in the second step (**II**). In the next step, the presence of a properly oriented C-H bond close to the metal center could lead to an electrophilic attack on the carbon atom of the phenyl ring with concomitant formation of a Wheland intermediate (**III**) [22]. The proposed electrophilic substitution is supported by the elimination of HCl during the cyclometalation, which is unique feature of the electrophilic pathway [24].

2.2. Characterization of the complexes

The infrared spectra of all ligands and ruthenium complexes have been recorded. The ligands exhibit significant bands around 1439–1427 and 1278–1267 cm^{-1} which are tentatively assigned to $\nu_{(N=N)}$ and phenolic $\nu_{(C-O)}$ stretching modes, respectively. On complexation, $\nu_{(N=N)}$ appears at 1395–1385 cm^{-1} and this red shift supports the coordination of azo-N to the metal center [25]. The coordination of metal ion to phenolic oxygen is confirmed by the increase of $\nu_{(C-O)}$ in the region 1308–1281 cm^{-1} when compared to free ligand. The positive shift is further supported by the disappearance of the $\nu_{(OH)}$ band in the range 3450–3430 cm^{-1} in all

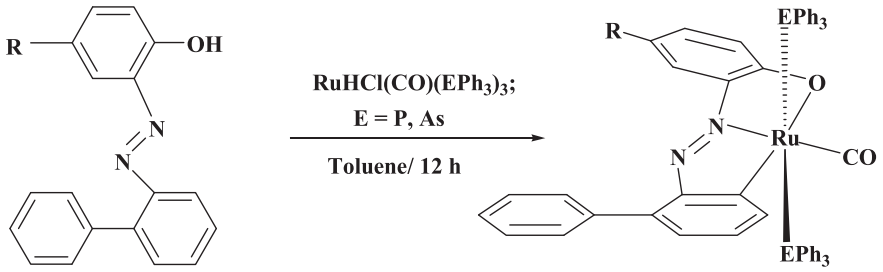

R = CH_3 (H_2L_1), OCH_3 (H_2L_2), $(CH_3)_3C$ (H_2L_3), Cl (H_2L_4)

R	E	Complexes
CH_3 (L_1)	E = P, As	1, 5
OCH_3 (L_2)	E = P, As	2, 6
$(CH_3)_3C$ (L_3)	E = P, As	3, 7
Cl (L_4)	E = P, As	4, 8

Scheme 1. Synthesis of cyclometalated Ru(II) 2-(biphenylazo)phenolate complexes **1**–**8**.

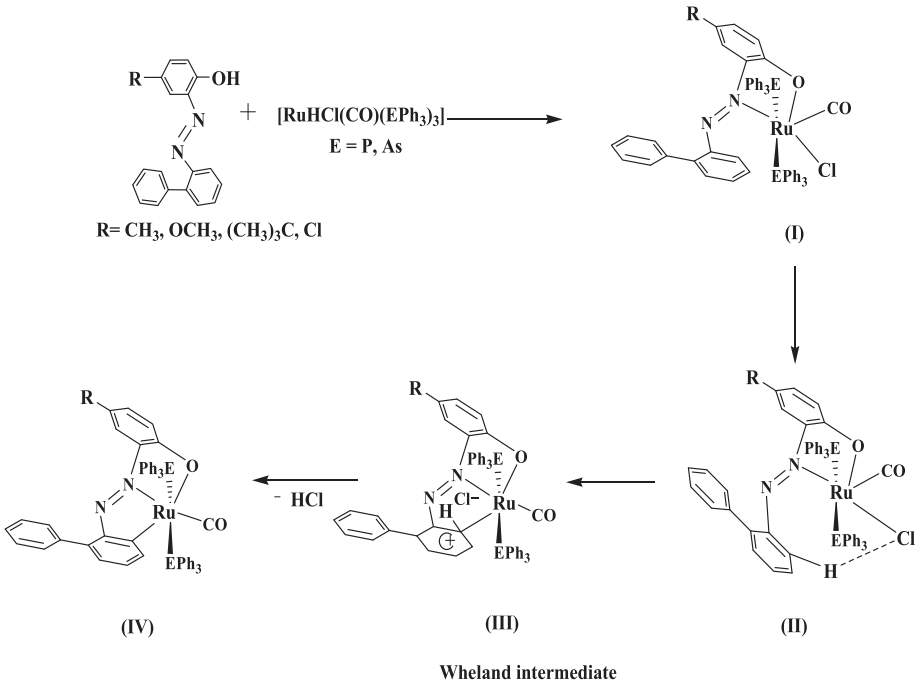

Scheme 2. Proposed mechanism for C-H activation.

complexes. The spectrum of each complexes shows a strong band in the region 1931–1924 cm^{-1} due to the coordinated carbonyl group [26,27]. The representative FT-IR spectra of complexes **1**–**8** are given in Figs. S1–S8 (ESI†). Further, these complexes show a strong band near 690, 740 and 1555 cm^{-1} indicating the presence of coordinated PPh_3 or $AsPh_3$ ligands [27].

In order to ascertain the nature of coordination mode of the crystallized complexes, we have computed the vibrational frequencies of five complexes using B3LYP functional. All the computed vibrational frequencies reported here are scaled with the scaling factor of 0.931. Particularly, our computed symmetric stretching carbonyl bands are consistent with the experimental vibrational frequency which appears in the region of 1929.9–1935.7 cm^{-1} in Table S9 (ESI†). For complex **4**, symmetric stretching frequencies of phenolic C_{Ph}—O group was observed at 1281 cm^{-1}. This particular vibration is affected by changing the *para*-substituent on the phenolate group. This vibration band is blue shifted upon introduction of the electron donating substituents such as methyl and *tert*-butyl. This effect is predominant for complex **1** which possess C_{Ph}—O band at 1333.2 cm^{-1}. The symmetric stretching vibration of Ru-PPh_3 bond $\nu_{Ru\text{-}X}$ of triphenylphosphine containing complexes such as **1**, **3** and **4** were observed between 503.8 cm^{-1} and 515.8 cm^{-1}. On the other hand, this particular vibrational frequency appears at 320.3 cm^{-1} and 313.4 cm^{-1} for the arsine containing complexes **5** and **7**.

The ^1H NMR spectra of the ruthenium(II) complexes have been recorded in $CDCl_3$ solution. All the complexes show multiplets around δ = 7.1–7.5 ppm due to the coordinated PPh_3/$AsPh_3$ ligands. Most of the expected aromatic proton signals for the coordinated 2-(biphenylazo)phenolate ligand, could not be detected due to their overlap with the PPh_3/$AsPh_3$ signals. The distinct methyl resonance is displayed for the complexes **1** and **5** at near δ = 1.80 and δ = 1.78 ppm respectively for *para*-cresol fragment of 2-(biphenylazo)phenolate ligands. A sharp singlet corresponding to the

methoxy protons is observed for complexes **2** and **6** at δ = 3.90 and δ = 3.89 ppm, respectively. The *tert*-butyl signals are also observed as singlets for complexes **3** and **7** at δ = 1.00 and δ = 0.99 ppm. Further, a sharp singlet appeared for the hydroxyl proton of all 2-(biphenylazo)phenol derivatives in the region around δ = 11.9–11.7 ppm, which is absent in all ruthenium complexes. In the ^{31}P NMR spectra of the complexes (**1**–**4**), a sharp singlet peak was observed in the region δ = 29.61–24.35 which confirm that the two triphenylphosphine group is coordinated to ruthenium in the complexes. Relevant ^{1}H NMR and ^{31}P NMR spectral data are collected in the experimental section and all spectra are provided in Figs. S10–S25 (ESI†). The ^{1}H NMR and FT-IR spectral data of the complexes are therefore consistent with the proposed structures (Scheme 1).

The UV-Vis spectra of all complexes in chloroform solutions exhibit characteristic absorptions in the region 200–800 nm. The representative UV-Vis spectra of complexes **1**-**8** are given in Figs. S26–S33 (ESI†). The absorption bands around 457–450 nm for all the complexes are assigned to Ru(dπ)-to-L($\pi*$) metal-to-ligand charge transfer (MLCT) transitions [28]. The lowest energy electronic spectral bands at around 760–740 nm are assigned to d-d transitions. The high intensity bands around 330–320 nm and 270–250 nm has been designated as n–$\pi*$ and π–$\pi*$ transitions respectively for the 2-(biphenylazo)phenolate ligands in these complexes. The obtained electronic spectral pattern of all complexes clearly shows the presence of an octahedral environment around the ruthenium(II) ion which is consistent with other reported ruthenium octahedral complexes [29,30].

2.3. X-ray structures

The molecular structure of complexes [Ru(L_1)(CO)(PPh_3)$_2$] (**1**), [Ru(L_3)(CO)(PPh_3)$_2$] (**3**), [Ru(L_4)(CO)(PPh_3)$_2$] (**4**), [Ru(L_1)(CO)($AsPh_3$)$_2$] (**5**) and [Ru(L_3)(CO)($AsPh_3$)$_2$] (**7**) was confirmed by single-crystal X-ray structure analysis. Despite the presence of acetonitrile molecules in the crystal packing of complexes **3** and **7**, which are therefore isolated as solvated compounds, all complexes are isostructural, showing the same arrangement of the ligands around the metal center. As expected, the triphenylphosphine/triphenylarsine ligands are axial in all complexes, while the C≡O and 2-(biphenylazo)phenolate ligands are coplanar. The molecular structures of the complexes are presented in Fig. 3. The crystallographic data and structural refinement parameters are given in Table S34 (ESI†). The formation of five-membered chelate rings upon coordination of the CNO- donor ligand imposes important distortions around the ruthenium atoms. The O-Ru-N (~78°) and C-Ru-N (~77°) angles are significantly smaller than 90°. Similarly, all C-Ru-O angles are comprised between 154.3(2) in **4** and 155.5 (1) in **7**, being far from the expected 180° of an ideal octahedral geometry. In all complexes, the equatorial plane formed by the phenylazophenolate moiety, the ruthenium atom, and the C≡O ligand is planar, with very small average deviations from an ideal plane (0.045 Å in **1**, 0.083 in **3**, 0.046 in **4**, 0.050 in **5**, 0.061 in **7**). In the crystal packing of **3** CH_3CN and **7** CH_3CN, there is no meaningful interaction between the complex and the acetonitrile molecule.

2.4. Redox properties

The electron transfer property of complexes **1**, **2**, **3** and **4** were studied in dichloromethane solutions by cyclic voltammetry techniques under N_2 atmosphere using a glassy-carbon working electrode and the redox potentials are expressed with reference to SCE. All these complexes (1×10^{-3} M) are electro-active with respect to the metal centers and exhibited three redox process in the potential range +1.6 V to −1.6 V. These complexes display a two quasi-reversible oxidative (Ru^{IV}/Ru^{III}); (Ru^{III}/Ru^{II}) and one quasi-reversible reductive (Ru^{II}/Ru^{I}) response on the positive and negative side of SCE respectively, at the scan rate of 100 mV s^{-1}. The potentials are summarized in Table 1 and the cyclic voltammogram of representative complexes is shown in Fig. 4. The comparison of its current height (i_{pa}) with that of the standard

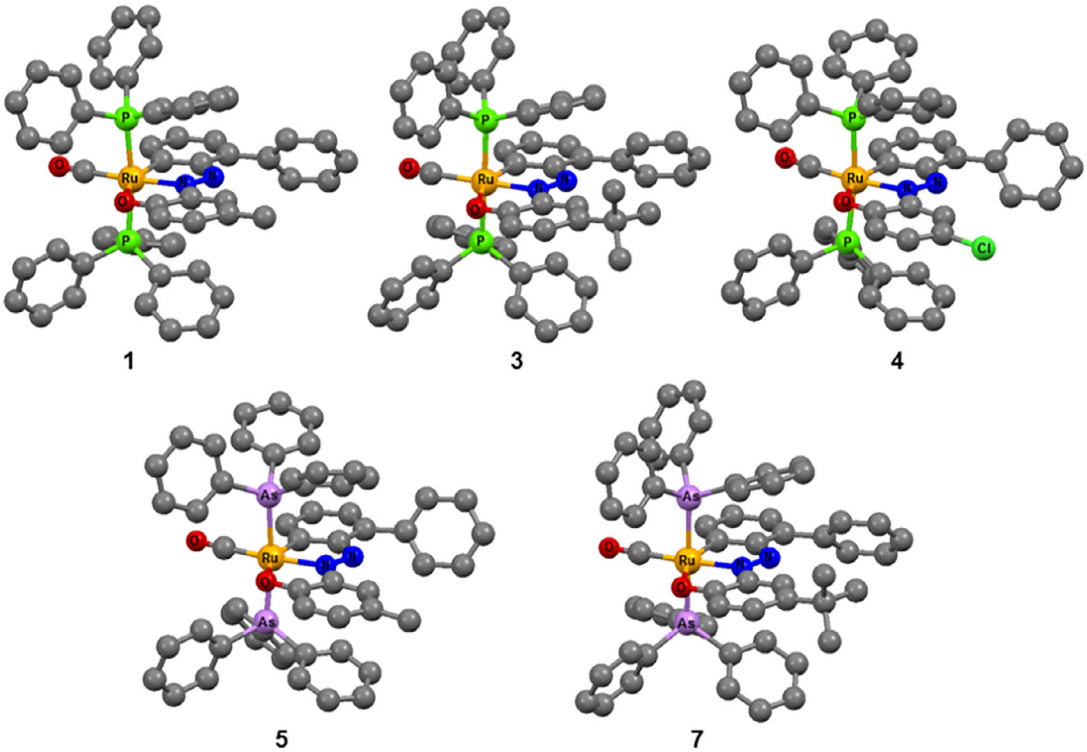

Fig. 3. X-ray structures of complexes **1**, **3**, **4**, **5**, and **7**, with hydrogen atoms and solvent molecules being omitted for clarity.

Table 1
Electrochemical data of ruthenium(II) 2-(biphenylazo)phenolate complexes **1**–**4**.

Complexes	Ru^{IV}/Ru^{III}				Ru^{III}/Ru^{II}				Ru^{II}/Ru^{I}			
	E_{pa} (V)	E_{pc} (V)	$E_{1/2}$ (V)	ΔE_p (mV)	E_{pa} (V)	E_{pc} (V)	$E_{1/2}$ (V)	ΔE_p (mV)	E_{pc} (V)	E_{pa} (V)	$E_{1/2}$ (V)	ΔE_p (mV)
1	1.01	0.83	0.92	181	0.78	0.48	0.63	298	−0.60	−0.50	−0.55	107
2	1.19	0.98	1.14	211	0.73	0.38	0.56	349	−0.63	−0.44	−0.53	187
3	1.06	0.83	0.94	230	0.80	0.44	0.62	353	−0.64	−0.45	−0.55	195
4	1.15	0.95	1.05	199	0.82	0.55	0.69	262	−0.56	−0.39	−0.47	162

Supporting electrolyte: NBu_4ClO_4 (0.005 M); complex: 0.001 M; solvent: CH_2Cl_2; $\Delta E_p = E_{pa} - E_{pc}$ where E_{pa} and E_{pc} are anodic and cathodic potentials respectively; $E_{1/2} = 0.5 (E_{pa} + E_{pc})$; scan rate: 100 mV s^{-1}.

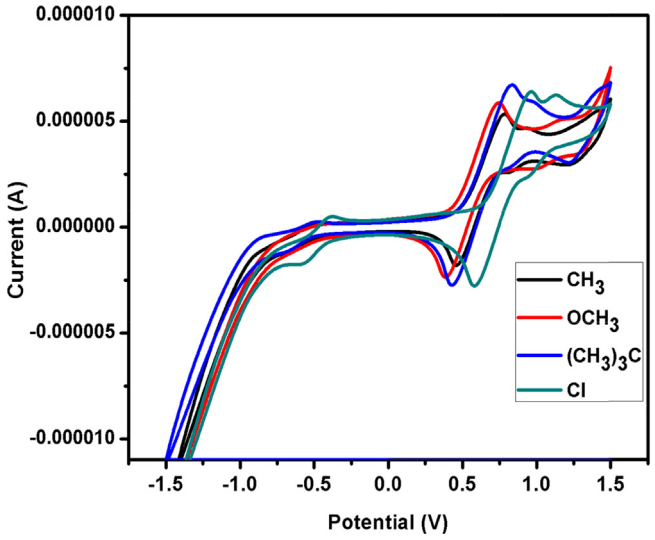

Fig. 4. Cyclic voltammogram of the complexes **1**–**4** in CH_2Cl_2 solutions (0.005 M TBAP) at the scan rate of 100 mV s^{-1}.

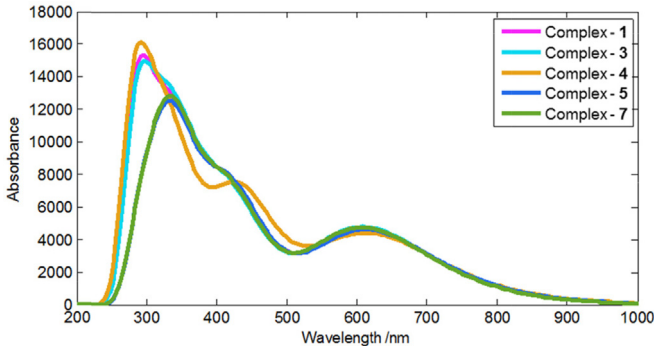

Fig. 5. B3LYP computed absorption spectrum of the complexes **1**, **3**, **4**, **5** and **7**.

ferrocene/ferrocenium couple under identical conditions, reveals the one electron redox process [31,32]. The well-defined reduction waves with $E_{1/2}$ in the range of −0.47 to −0.55 V is assigned to $Ru^{II} \rightarrow Ru^{I}$ reduction [33,34]. The redox processes are quasi-reversible in nature, characterized by a rather large peak-to-peak separation (ΔE_p) of 107–195 mV. The reduction potentials for the Ru(II)/Ru(I) couples are expected to respond to both (σ) donor and (π) acceptor properties of the ligands. The acceptor properties are important in terms of stabilization of Ru(I) while donor properties of ligands probably lead to stabilization of Ru(II).

The second quasi-reversible oxidation couple Ru(IV)/Ru(III) observed in these complexes which could be due to phosphine localized oxidation. The first irreversible oxidative response with $E_{1/2}$ in the range + 0.56 to + 0.69 V was assigned to $Ru^{II} \rightarrow Ru^{III}$ oxidation, whereas the second irreversible oxidation response with $E_{1/2}$ in the range +0.92 to 1.14 V was assigned to $Ru^{III} \rightarrow Ru^{IV}$ oxidation state. The potentials are comparable with $Ru^{II} \rightarrow Ru^{III}$ and $Ru^{III} \rightarrow Ru^{IV}$ oxidation potentials of other ruthenium complexes [35,36]. The irreversibility observed for the oxidative response may be due to the fast dissociation of PPh_3/$AsPh_3$ from these ruthenium(II) complexes [37,38].

2.5. Electronic structure calculations

Detailed quantum chemical calculations were performed on the effect of methyl, methoxy, *tert*-butyl and chloro groups on the 2-(biphenylazo)phenolate ligand of cyclometalated ruthenium(II) complexes with triphenylphosphine and triphenylarsine ligands. Among the eight complexes, three triphenylphosphine containing cyclometalated ruthenium(II) complexes **1, 3,** and **4** and two triphenylarsine containing cyclometalated ruthenium(II) complexes **5** and **7** were crystallized. Preliminary geometrical information of all the five complexes were obtained from X-ray crystallized coordinates. Cyclometalated ruthenium(II) complexes are found to possess the singlet spin ground state with the fundamental $(d_{xy})^2 (d_{xz})^2 (d_{yz})^2 (d_z^2)^0 (d_{x^2-y^2})^0$ electronic configuration. All the five complexes were attributed with similar kind of electronic configurations.

Notable geometrical parameters obtained from DFT and X-ray crystallographic methods are given in Table S35 (ESI†). In this work, we have used B3LYP functional for calculating structural and spectroscopic aspects of the five different complexes under investigation. The reliability of B3LYP functional is already well documented from earlier reports [25,55] on predicting the structural parameters. Our computed structural parameters are in good agreement with the X-ray crystallized bond parameters. The presence of ancillary ligands such as PPh_3 and $AsPh_3$ were found to have significant role on stabilizing the Ru-C(Ar) bond. Upon analyzing structural parameters of all the five complexes, they were found to have distorted octahedral sphere.

2.6. TD-DFT calculations

In order to understand the nature of electronic excitations, time dependent density functional theory (TD-DFT) calculations were performed for the five crystallized complexes (**1**, **3**, **4**, **5** and **7**) using SCRF-PCM chloroform continuum. The calculated wavelength of maxima, excitation energies, oscillator strength along with nature of electronic transition and simulated absorption spectra are provided in Fig. 5 and Table S36 (ESI†). Among the many possible transitions, only those absorption bands with oscillator strength (f) > 0.1 would be considered for the present discussion. As similar to the experimental observations, TD-DFT calculations also predict the similar absorption bands for the five complexes studied here. All the five complexes were found to have four major absorption bands. Among the five complexes, triphenylphosphine containing ruthenium complexes such as **1**, **3** and **4** were found

to have most intense absorption bands in the region of 283.7 nm, 284.5 nm and 279.2 nm with the oscillator strength of 0.214, 0.194 and 0.214 respectively. While the triphenylarsine containing complexes such as **5** and **7** were found to have less intense absorption bands of 293.5 nm and 293.9 nm with low oscillator strength of 0.030 and 0.029. This is clearly inferred from the frontier molecular orbitals (See Figs. 6 and 7) involving four major absorption bands of complex **4** and **7**. This particular absorption bands could be helpful to distinguish the role of PPh_3 and $AsPh_3$ ligands in the ruthenium complexes [25a,b].

Upon investigation of NTO orbitals of relevant transitions of complexes **4** and **7** (Fig. 8 and Table S36 (ESI†) the nature of the electronic transition is purely different and it is mainly originated from the excitation of electron from the 2-(biphenylazo)phenolate ligand to triphenylphosphine ligand along with the small contribution from Ru-d_z^2 orbital in complex **4**. In contrast, the excitation in complex **7** occurs from the filled t_{2g} orbital of ruthenium with some contribution from 2-(biphenylazo)phenolate ligand to triphenyarsine ligands. The lowest energy with less intense transition for complex **4** was observed at 619.5 nm with oscillator strength of 0.107. This absorption bands is slightly blue shifted by changing the different substituents on the *para*-position of the phenolate group. Similarly, other two transitions lies at 437.2 nm and 328.6 nm were MLCT in nature. All the other complexes were found to have similar kind of trend.

2.7. Catalytic activity

Ruthenium mediated oxidation reactions are finding increasing application due to the unique properties of this extremely versatile transition metal, whose oxidation state can vary from −2 to +8 and prompted us to carry out this type of reaction. The catalytic oxidation of secondary alcohols into ketones was performed by using the complexes $[Ru(L_{1-4})(CO)(PPh_3)_2]$ (**14**) (1 mol%) as catalysts. These complexes effectively catalyze the oxidation of aromatic and aliphatic secondary alcohols such as benzhydrol, cyclohexanol and 1-phenylethanol into their corresponding ketones with high conversion up to 99%, the results are listed in Table 2.

It has been observed that the ruthenium complexes show high catalytic efficiency in low catalyst loading and yield is good when compared to other ruthenium complexes as catalysts in the presence of *N*-methylmorpholine-*N*-oxide/*tert*-butyl hydroperoxide as reported earlier [12,39–42]. The present ligand system in the complexes stabilizes the higher oxidation state which is inferred from the electrochemical studies. Moreover, the ligand system plays a significant role due to steric and electronic environment at the ruthenium metal center. It is also noted that the substituents on phenolic group does not have influence in the catalytic conversion. The probable mechanism for the observed oxidation of alcohols to ketones follows the classical pathway as in Scheme 3.

Transfer hydrogenation of acetophenone in the presence of cyclometalated ruthenium(II) 2-(biphenylazo)phenolate complexes as catalysts have been studied in *i*-PrOH/KOH medium. The reactions were conducted at a catalyst, substrate and base (C/S/base) in 1:500:2.5 M ratios. In order to optimize the reaction conditions, different catalyst: substrate (C/S) mole ratios (1:500; 1:1000 & 1:1500) were tested and the results summarized in Table 3. For this initial experiments, acetophenone was selected as a test substrate and allowed to react with catalytic quantity of $[Ru(L_1)(CO)(PPh_3)_2]$ (**1**) in the presence of *i*-PrOH/KOH. When increasing the C/S ratio to 1:1000, 1:1500 in *i*-PrOH, the reaction still proceeds with reasonable conversions. It was concluded that the catalyst: substrate ratio of 1:500 was the best compromise between optimum reaction rate and C/S ratio. It was also observed that these complexes did not result in the transfer hydrogenation of acetophenone in the absence of base.

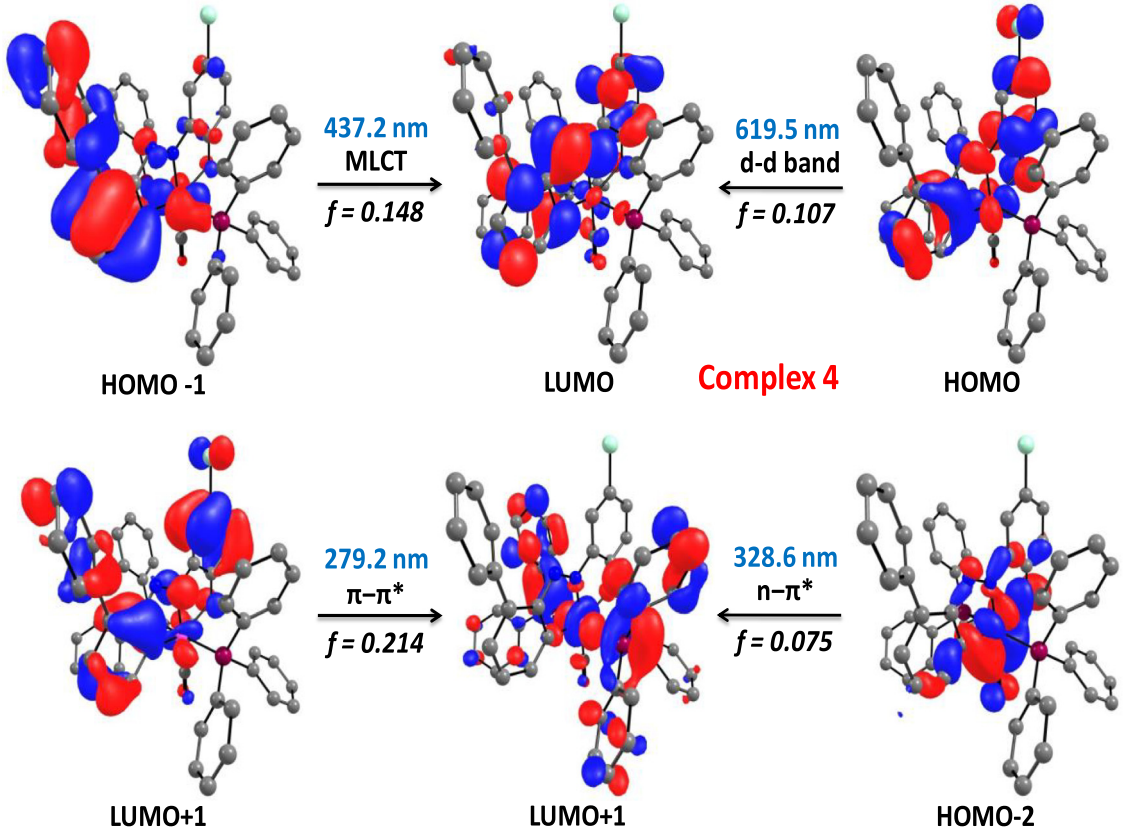

Fig. 6. Frontier molecular orbitals of four major absorption bands of complex **4**.

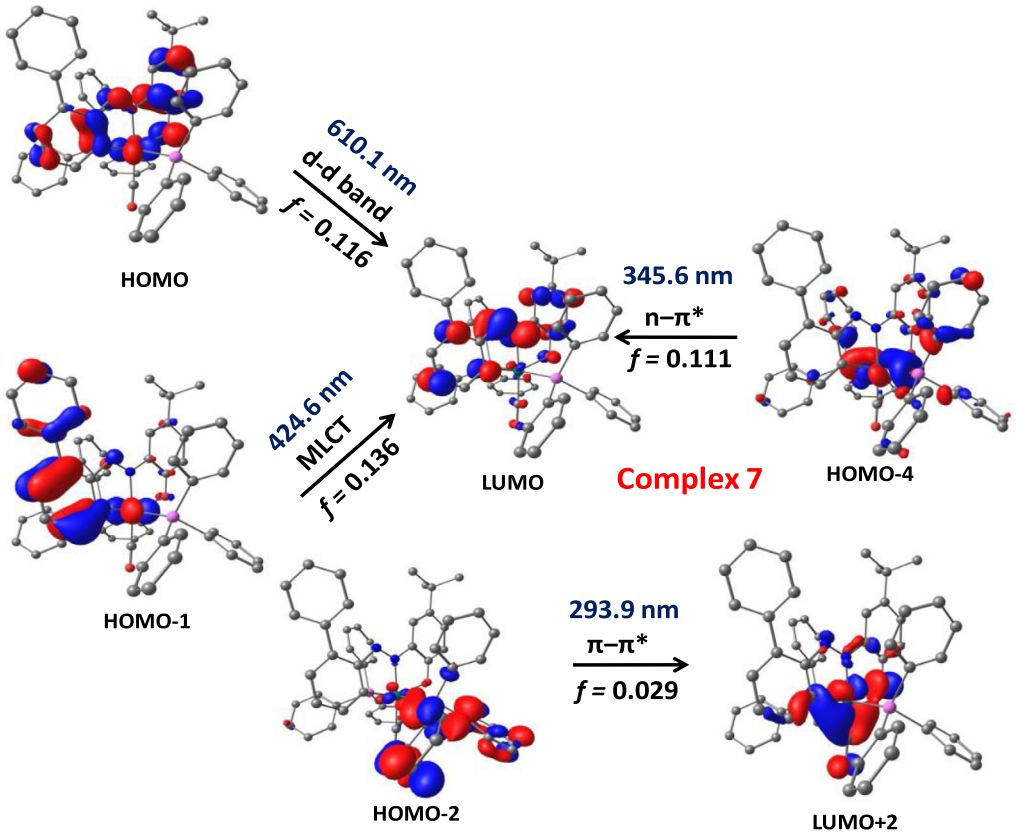

Fig. 7. Frontier molecular orbitals of four major absorption bands of complex **7**.

Complex	λ_{max}	*f*	NTO Hole	NTO Particle
4	279.2 nm	0.214	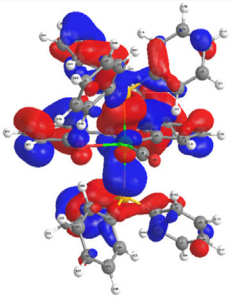	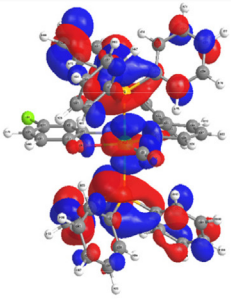
7	424.6 nm	0.136	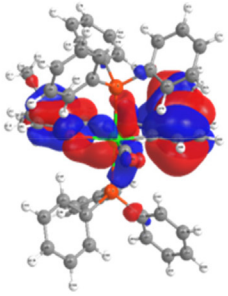	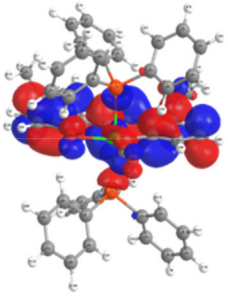

Fig. 8. Natural transition orbitals (NTOs) of intense absorption band for complexes **4**, and **7** shown on occupied (holes) and unoccupied (electrons) NTO pairs.

The catalysts performed efficiently for aromatic and aliphatic ketones with high conversion and the results are shown in Table 4. In most cases, the ketone substrate was converted into corresponding alcohol up to 99%. Similarly, cyclohexanone was converted to cyclohexanol up to 92%. The conversion of acetophenone into 1-phenylethanol was completed with 99%. Low catalyst loading

Table 2
Catalytic oxidation of alcohols using complexes **1**-**4**[a].

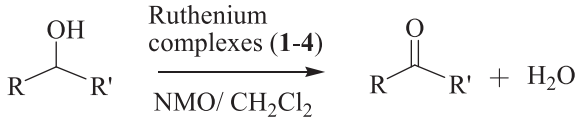

Complex	Substrate	Product	Conv. (%)	TON[b]
1	Benzhydrol	Benzophenone	99	99
	1-Phenylethanol	Acetophenone	87	87
	Cyclohexanol	Cyclohexanone	93	93
2	Benzhydrol	Benzophenone	98	98
	1-Phenylethanol	Acetophenone	89	89
	Cyclohexanol	Cyclohexanone	91	91
3	Benzhydrol	Benzophenone	97	97
	1-Phenylethanol	Acetophenone	93	93
	Cyclohexanol	Cyclohexanone	96	96
4	Benzhydrol	Benzophenone	95	95
	1-Phenylethanol	Acetophenone	92	92
	Cyclohexanol	Cyclohexanone	89	89

Conversion was determined by GC analysis with authentic samples.
[a] Substrate (1 mmol); *N*-methylmorpholine-*N*-oxide (NMO) (3 mmol); complex (0.01 mmol); solvent: dichloromethane; Temp. 40 °C; Reaction after 2 h.
[b] TON = ratio of moles of product obtained to the moles of the catalyst used.

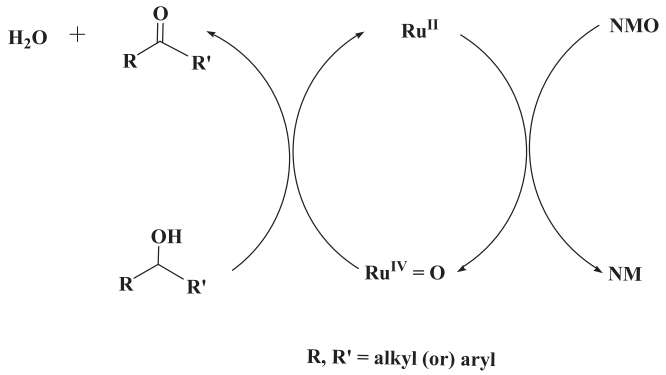

Scheme 3. Proposed catalytic cycle for the oxidation of alcohols by ruthenium(II) complexes.

Table 3
Catalytic transfer hydrogenation of acetophenone using complex **1**[a].

Entry	C/S	Time (h)	Conversion (%)	TON[b]
1	1:1500	2	75	1125
2	1:1000	2	84	840
3	1:500	2	99	495

Conversion was determined by GC analysis with authentic samples.
[a] Conditions: reactions were carried out at 80 °C using acetophenone (5–15 mmol), catalyst (0.002 mmol) in 10 mL of *i*-PrOH and KOH (0.005 mmol) for 2 h.
[b] TON = ratio of moles of product obtained to the moles of the catalyst used.

was enough to achieve up to 99%. The present catalytic loading, temperature adopted was quite low and the yield was also good when compared with other catalytic systems [16]. The base facilitated the formation of the ruthenium alkoxide by abstracting the proton from alcohol and subsequently, the alkoxide underwent β-elimination to give a ruthenium hydride which is the active species in this reaction [19]. Although several catalytic systems have been reported to support transfer hydrogenation reaction of ketones, catalysts of this type are new for its CNO- donor, PPh_3 and CO ligand environment. The unsymmetrical environment around the metal center in the complexes is crucial to the good catalytic activity of the complexes due to the precise control of their electronic and geometric properties. The presence of two bulky triphenylphosphine ligands in these complexes results in labile molecular structures and thus leads to a higher catalytic activity for the transfer hydrogenation of ketones. The electronic nature of the substituents in the 2-(biphenylazo)phenol ligands has no measurable influence on the catalytic activity of these ruthenium complexes.

3. Conclusions

Reactions between *para*-substituted 2-(biphenylazo)phenol ligands with ruthenium(II) precursors have been carried out to prepare a family of cyclometalated ruthenium(II) carbonyl complexes. The structure of these complexes were elucidated by spectral and X-ray diffraction studies. The redox behavior of the complexes was also studied by cyclic voltammetry techniques. Our computed results are in good agreement with experimental data. TD-DFT calculations clearly pinpoint the nature of electronic transitions involved in these cyclometalated ruthenium(II) complexes. These ruthenium complexes turned out to be versatile catalysts for both, the oxidation of alcohols and the transfer hydrogenation of ketones.

4. Experimental procedure

4.1. Materials and reagents

All the reagents used were chemically pure and of analytical grade. The solvents were freshly distilled before use. $RuCl_3{\cdot}3H_2O$ was purchased from Himedia Pvt. Ltd., and was used without further purification. The 2-aminobiphenyl was purchased from Aldrich. The starting precursor complexes $[RuHCl(CO)(PPh_3)_3]$ [43] and $[RuHCl(CO)(AsPh_3)_3]$ [44] were prepared according to the literature reports. The 2-(biphenylazo)phenol ligands [45] were prepared by diazotization reaction of 2-aminobiphenyl with corresponding *para*-substituted phenols.

4.2. Physical measurements

‘ The microanalysis of carbon, hydrogen and nitrogen was carried out using a Vario EL III Elemental analyzer at SAIF – Cochin,

Table 4
Catalytic transfer hydrogenation of ketones using complexes **1–4**[a].

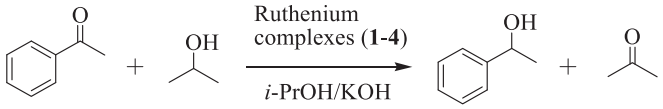

Complex	Substrate	Product	Conv. (%)	TON[b]
1	Benzophenone	Benzhydrol	99	495
	Acetophenone	1-Phenylethanol	99	495
	Cyclohexanone	Cyclohexanol	90	450
2	Benzophenone	Benzhydrol	93	465
	Acetophenone	1-Phenylethanol	98	490
	Cyclohexanone	Cyclohexanol	89	445
3	Benzophenone	Benzhydrol	97	485
	Acetophenone	1-Phenylethanol	89	445
	Cyclohexanol	Cyclohexanol	92	460
4	Benzophenone	Benzhydrol	97	485
	Acetophenone	1-Phenylethanol	86	430
	Cyclohexanone	Cyclohexanol	99	495

Conversion was determined by GC analysis with authentic samples.
[a] Conditions: reactions were carried out at 80 °C using 1 mmol of ketone (5 mL *i*-PrOH); catalyst/ketone/KOH ratio is 1:500: 2.5 for 2 h.
[b] TON = ratio of moles of product obtained to the moles of the catalyst used.

India. The IR spectra of the complexes were recorded on an agilent resolution pro model in 4000–400 cm^{-1} range. Electronic spectra of the complexes were recorded in $CHCl_3$ solution in a Cary 300 Bio UV-Vis Varian spectrophotometer in the range 800–200 nm. The ^1H NMR spectra were recorded in $CDCl_3$ with Bruker 300 MHz instrument using TMS as internal reference. Electrochemical measurements were made using CHI608E electrochemical analyzer. A three electrode cell was employed with glassy carbon working electrode, a platinum wire counter electrode and an Ag/AgCl reference electrode in the cyclic voltammetry experiments. All electrochemical experiments were performed under N_2 atmosphere. All electrochemical data were collected at 298 K and uncorrected for junction potentials. Melting point was recorded in the Boeties micro heating table and uncorrected.

4.3. General procedure for the synthesis of complexes *1-8*

To a toluene solution of $[RuHCl(CO)(EPh_3)_3]$ (E = P, As) (100 mg; 0.1 mmol) were added the appropriate ligands (H_2L_1–H_2L_4) (0.1 mmol) and the mixtures were refluxed for 12 h. The color of the reaction mixtures changed gradually and the reactions were monitored by TLC. The solution was concentrated to about 3 mL and 10 mL of petroleum ether (60–80 °C) was added to precipitate green colored solids, which were isolated by filtration. The crude products were purified by column chromatography using chloroform as eluent. On evaporation of the solution, the pure ruthenium complexes were obtained as crystalline solids with good yields.

4.3.1. $[Ru(L_1)(CO)(PPh_3)_2]$ (*1*)
Yield: 65%; green solid; M.p. 202 °C, Anal. Calc. for $C_{56}H_{44}N_2O_2P_2Ru$: C, 71.33; H, 4.67; N, 2.97; Found: C, 71.02; H. 4.22; N, 2.83. FT-IR (cm^{-1}): 1929 $\nu_{(C\equiv O)}$, 1392 $\nu_{(N=N)}$, 1301 $\nu_{(C\text{-}O)}$. ^1H NMR (300 MHz, $CDCl_3$): δ (ppm) = 7.1–7.95 (m, Ar-H), 1.80 (s, CH_3). ^{31}P NMR δ = 29.13. UV-Vis λ_{max} (nm): 745, 450, 325, 250.

4.3.2. $[Ru(L_2)(CO)(PPh_3)_2]$ (*2*)
Yield: 68%; green solid; M.p. 206 °C, Anal. Calc. for $C_{56}H_{44}N_2O_3P_2Ru$: C, 70.14; H, 4.59; N, 2.92; Found: C, 70.01; H. 4.06; N, 2.63. FT-IR (cm^{-1}): 1929 $\nu_{(C\equiv O)}$, 1394 $\nu_{(N=N)}$, 1318 $\nu_{(C\text{-}O)}$. ^1H NMR (300 MHz, $CDCl_3$): δ (ppm) = 7.2–7.50 (m, Ar-H), 3.90 (s, OCH_3). ^{31}P NMR δ = 24.35. UV-Vis λ_{max} (nm): 750, 450, 325, 255.

4.3.3. $[Ru(L_3)(CO)(PPh_3)_2]$ (*3*)
Yield: 62%; green solid; M.p. 201 °C, Anal. Calc. for $C_{59}H_{50}N_2O_2P_2Ru$: C, 71.88; H, 5.07; N, 2.84; Found: C, 71.47; H. 4.98; N, 2.79. FT-IR (cm^{-1}): 1931 $\nu_{(C\equiv O)}$, 1390 $\nu_{(N=N)}$, 1308 $\nu_{(C\text{-}O)}$. ^1H NMR (300 MHz, $CDCl_3$): δ (ppm) = 7.1–7.55 (m, Ar-H), 1.00 (s, $(CH_3)_3C$). ^{31}P NMR δ = 24.35. UV-Vis λ_{max} (nm): 750, 455, 330, 260.

4.3.4. $[Ru(L_4)(CO)(PPh_3)_2]$ (*4*)
Yield: 60%; green solid; M.p. 190 °C, Anal. Calc. for $C_{55}H_{41}Cl_1N_2O_2P_2Ru$: C, 68.51; H, 4.25; N, 2.90; Found: C, 68.12; H. 4.06; N, 2.73. FT-IR (cm^{-1}): 1930 $\nu_{(C\equiv O)}$, 1391 $\nu_{(N=N)}$, 1311 $\nu_{(C\text{-}O)}$. ^1H NMR (300 MHz, $CDCl_3$): δ (ppm) = 7.0–7.50 (m, Ar-H). ^{31}P NMR δ = 29.61. UV-Vis λ_{max} (nm): 745, 455, 320, 260.

4.3.5. $[Ru(L_1)(CO)(AsPh_3)]$ (*5*)
Yield: 70%; green solid; M.p. 195 °C, Anal. Calc. for $C_{56}H_{44}N_2O_2As_2Ru$: C, 65.42; H, 4.28; N, 2.72; Found: C, 65.13; H. 4.03; N, 2.59. FT-IR (cm^{-1}): 1924 $\nu_{(C\equiv O)}$, 1391 $\nu_{(N=N)}$, 1300 $\nu_{(C\text{-}O)}$. ^1H NMR (300 MHz, $CDCl_3$): δ (ppm) = 7.1–7.60 (m, Ar-H), 1.85 (s, CH_3). UV-Vis λ_{max} (nm): 750, 455, 330, 270.

4.3.6. $[Ru(L_2)(CO)(AsPh_3)_2]$ (*6*)
Yield: 75%; green solid; M.p. 203 °C, Anal. Calc. for $C_{56}H_{44}N_2O_3As_2Ru$: C, 64.42; H, 4.21; N, 2.68; Found: C, 63.97; H. 4.05; N, 2.22. FT-IR (cm^{-1}): 1930 $\nu_{(C\equiv O)}$, 1395 $\nu_{(N=N)}$, 1319 $\nu_{(C\text{-}O)}$. ^1H NMR (300 MHz, $CDCl_3$): δ (ppm) = 7.0–7.65 (m, Ar-H), 3.91 (s, OCH_3). UV λ_{max} (nm): 750, 455, 330, 265.

4.3.7. $[Ru(L_3)(CO)(AsPh_3)_2]$ (*7*)
Yield: 69%; green solid; M.p. 187 °C, Anal. Calc. for $C_{59}H_{50}N_2O_2As_2Ru$: C, 66.22; H, 4.67; N, 2.61; found: C, 65.98; H. 4.09; N, 2.21. FT-IR (cm^{-1}): 1928 $\nu_{(C\equiv O)}$, 1385 $\nu_{(N=N)}$, 1306 $\nu_{(C\text{-}O)}$. ^1H NMR (300 MHz, $CDCl_3$): δ (ppm) = 7.1–7.40 (m, Ar-H), 0.99 (s, $(CH_3)_3C$). UV–Vis λ_{max} (nm): 760, 450, 320, 270.

4.3.8. $[Ru(L_4)(CO)(AsPh_3)_2]$ (*8*)
Yield: 60%; green solid; M.p. 196 °C, Anal. Calc. for $C_{55}H_{41}Cl_1N_2O_2As_2Ru$: C, 63.00; H, 3.91; N, 2.67; found: C, 62.87; H. 3.19; N, 2.13. FT-IR (cm^{-1}): 1925 $\nu_{(C\equiv O)}$, 1388 $\nu_{(N=N)}$, 1299 $\nu_{(C\text{-}O)}$. ^1H NMR (300 MHz, $CDCl_3$): δ (ppm) = 7.1–7.48 (m, Ar-H). UV-Vis λ_{max} (nm): 755, 450, 330, 270.

4.4. Catalytic oxidation

The catalytic oxidation of primary alcohols to corresponding aldehydes and secondary alcohols to ketones by cyclometalated ruthenium(II) complexes was studied in the presence of NMO as co-oxidant. A typical reaction using the complexes [Ru(L_{1-4})(CO)(PPh_3)$_2$] (**1**–**4**) as a catalysts and primary or secondary alcohol as substrates at a 1:100 M ratio was conducted as follows. A solution of ruthenium complexes (0.01 mmol) in 20 mL CH_2Cl_2 was added to the solution of substrate (1 mmol) and *N*-methylmorpholine-*N*-oxide (NMO) (3 mmol). The reaction mixture was refluxed for 2 h and the solvent was then evaporated from the mother liquor under reduced pressure. The residue was then extracted with petroleum ether (60–80 °C) (20 mL) and was analyzed by GC. The oxidation products were identified by GC co-injection with authentic samples.

4.5. Catalytic transfer hydrogenation of ketones

The catalytic transfer hydrogenation reactions were also studied using ruthenium(II) 2-(biphenylazo)phenolate complexes as a catalyst, ketone as substrate and KOH as base at 1:500:2.5 M ratio. The procedure adopted was as follows. A mixture containing ketone (1 mmol), the ruthenium complex (0.002 mmol) and KOH (0.03 mmol) was heated to reflux in 5 mL of *i*-PrOH for 2 h. After completion of the reaction, the catalyst was removed from the reaction mixture by the addition of petroleum ether (60–80 °C) followed by filtration and subsequent neutralization with 1 M HCl. The ether layer was filtered through a short path of silica gel by column chromatography. The filtrate was subjected to GC analysis and the hydrogenated product was identified and determined with authentic samples.

4.6. X-ray crystallography

Single crystals of the ruthenium complexes (**1**, **3** CH_3CN, **4**, **5**, and **7** CH_3CN) were obtained by slow diffusion at room temperature of acetonitrile in-to chloroform solutions of the corresponding complexes. Crystals were mounted on a Stoe Mark II-Image Plate Diffraction System, and analyzed using Mo-Kα graphite monochromated radiation, image plate distance 135 mm, 2θ range from 2.4 to 51.3°, D_{max}-D_{min} = 16.029–0.836 Å. The structures were solved by direct methods using the program SHELXS-97. [46] Refinement and all further calculations were carried out using SHELXL-97. The H-atoms were included in calculated positions and treated as riding atoms using the SHELXL default parameters. The non-H atoms were refined anisotropically, using weighted full-matrix least-square on F^2 [47].

4.7. Computational details

Quantum chemical calculations were performed using Gaussian 09 program [48] Unrestricted B3LYP [49,50] functional with a Los Alamos effective core potential double zeta valence basis set (LANL2DZ) [51,52] on Ru was used and 6-31G(d) basis set was used for rest of the atoms. The reliability of B3LYP functional in predicting electronic structure, absorption properties were already witnessed from earlier reports [53,54]. Time dependent density functional theory (TDDFT) implemented in the Gaussian 09 program was used for the calculation of excitation energies for first 50 states.

Acknowledgments

The authors express sincere thanks to Dr. J. Madhavan, Department of Chemistry, Thiruvalluvar University, Vellore, for cyclic voltammetric facilities. MDK thank Loyola College-Times of India (LC-TOI) Major Research Project (Ref. 2LCTOI14CHM001) for financial support and MJ thank LC-TOI for High-Performance Computing facilities.

Appendix A. Supplementary data

Supplementary data associated with this article can be found, in the online version, at https://doi.org/10.1016/j.ica.2018.02.023.

References

[1] (a) D.L. Davies, S.A. Macgregor, C.L. McMullin, Chem. Rev. 117 (2017) 8649; (b) J.-P. Djukic, J.-B. Sortais, L. Barloy, M. Pfeffer, Eur. J. Inorg. Chem. (2009) 817; (c) A.D. Ryabov, Chem. Rev. 90 (1990) 403.
[2] (a) D. Balcells, E. Clot, O. Eisenstein, Chem. Rev. 110 (2010) 749; (b) D. Lapointe, K. Fagnou, Chem. Lett. 39 (2010) 1119; (c) Y. Boutadla, D. L. Davies, S. A. Macgregor, A. I. Poblador- Bahamonde, Dalton Trans. 2009, 5820–5831.
[3] (a) L. Xiao, Z. Chen, B. Qu, J. Luo, S. Kong, Q. Gons, J. Kiod, Adv. Mater. 23 (2011) 926; (b) Q. Zhao, F. Li, C. Huang, Chem. Soc. Rev. 39 (2010) 3007; (c) J.W. Slater, J.P. Rourkee, J. Organomet. Chem. 688 (2003) 112.
[4] R. Drozdzak, B. Allaert, N. Ledoux, I. Dragutan, F. Verpoort, Coord. Chem. Rev. 249 (2005) 3055.
[5] S.V. Ley, J. Norman, W.P. Griffith, S.P. Marsden, Synthesis. (1994) 639.
[6] A. Hanyu, E. Takezwa, S. Sakaguchi, Y. Ishii, Tetrahedron Lett. 39 (1998) 5557.
[7] D. Chatterjee, A. Mitra, S. Mukherjee, J. Mol. Catal. A: Chem. 165 (2001) 295.
[8] S. Campestrini, M. Carraro, U. Tonellato, M. Pagliaro, R. Ciriminna, Tetrahedron Lett. 45 (2004) 7283.
[9] C. Bilgrien, S. Davis, R.S. Drago, J. Am. Chem. Soc. 109 (1987) 3786.
[10] P. Muller, J. Godoy, Tetrahedron Lett. 22 (1981) 2361.
[11] W.S. Trahanosky, Oxidation of Organic Chemistry, Academic Press, Part B, 1973.
[12] A.M. El-Hendawy, A.H. Alkubaisi, A.E. Kourashy, M.M. Shanab, Polyhedron 12 (1993) 2343.
[13] (a) M. Yoshimura, S. Tanaka, M. Kitamura, Tetrahedron Lett. 55 (2014) 3635; (b) N. Mohan, R. Ramesh, Appl. Organometal. Chem. (2016) 1; (c) D. Elma, F. Durap, M. Aydemir, A. Baysal, N. Meriç, B. Ak, Y. Turgut, B. Gümgüm, J. Organometal. Chem. 729 (2013) 46; (d) O. Dayan, N. Özdemir, Z. Şerbetçi, M. Dinçer, B. Çetinkaya, O. Büyükgüngör, Inorg. Chim. Acta. 392 (2012) 246; (e) J. Hannedouche, G.J. Clarkson, M. Wills, J. Am. Chem. Soc. 126 (2004) 986.
[14] (a) M. Kitamura, M. Yoshimura, N. Kanda, R. Noyori, Tetrahedron. 55 (1999) 8769; (b) M. Yamakawa, H. Ito, R. Noyori, J. Am. Chem. Soc. 122 (2000) 1466; (c) R. Noyori, T. Ohkuma, Angew Chem. Int. Ed. 40 (2001) 40.
[15] (a) M. Ramesh, G. Prabusankar, G. Venkatachalam, Inorg. Chem. Commun. 79 (2017) 89; (b) G. Venkatachalam, R. Ramesh, Tetrahedron Lett. 46 (2005) 5215.
[16] L. T. Ghoochany, S. Farsadpour, Y. Sun, W. R. Thiel, Eur. J. Inorg. Chem. (2011) 3431 and references there in.
[17] (a) J.B. Sortais, V. Ritleng, A. Voelklin, A. Holuigue, H. Smail, L. Barloy, C. Sirlin, G.K.M. Verzijl, J.A.F. Boogers, A.H.M. De Vries, J.G. De Vries, M. Pfeffer, Org. Lett. 7 (2005) 1247; (b) D. Amoroso, A. Jabri, G.P.A. Yap, D.G. Gusev, E.N. Dos Sanntos, D.E. Fogg, Organometallics 23 (2004) 4047.
[18] (a) J. Dutta, M.G. Richmond, S. Bhattacharya, Eur. J. Inorg. Chem. 27 (2014) 4600; (b) C. Guyon, E. Métay, N. Duguet, M. Lemaire, Eur. J. Org. Chem. (2013) 5439; (c) M.E. Cucciolito, B. Panunzi, F. Ruffo, A. Tuzi, Tetrahedron Lett. 54 (2013) 1503; (d) T.S. Manikandan, S. Saranya, R. Ramesh, Tetrahedron Lett. 57 (2016) 3764.
[19] W. Du, L. Wang, P. Wu, Z. Yu, Chem. Eur. J. 18 (2012) 11550.
[20] W. Baratta, M. Ballico, G. Chelucci, K. Siega, P. Rigo, Angew. Chem. Int. Ed. 47 (2008) 4362.
[21] (a) K. Siu, S.M. Peng, S. Bhattacharya, Polyhedron 18 (1999) 631; (b) P. Gupta, S. Dutta, F. Basuli, S.M. Peng, G.H. Lee, S. Bhattacharya, Inorg. Chem. 45 (2006) 460.
[22] (a) K. Ghosh, S. Kumar, R. Kumar, U.P. Singh, Eur. J. Inorg. Chem. (2012) 929; (b) N. Chitrapriya, V. Mahalingam, M. Zeller, K. Natarajan, Polyhedron 27 (2008) 1573; (c) R.L. Brainard, W.R. Nutt, T.R. Lee, G.M. Whitesides, Organometallics 7 (1998) 2379; (d) R. Cordone, W.D. Harman, H. Taube, J. Am. Chem. Soc. 111 (1989) 2896.
[23] (a) S. Cenini, F. Porta, M. Pizzotti, J. Mol. Catal. 15 (1982) 297; (b) A.A. Batista, M.O. Santiago, C.L. Donnici, I.S. Moreira, P.C. Healy, S.J. Berners-Price, S.L. Queiroz, Polyhedron 20 (2001) 2123; (c) M.I.F. Barbosa, R.S. Correa, K.M. de Oliveira, C. Rodrigues, J. Ellena, O.R. Nascimento, V.P.C. Rocha, F.R. Nonato, T.S. Macedo, J.M. Barbosa-Filho, M.B.P. Soares, A.A. Batista, J. Inorg. Biochem. 136 (2014) 33.
[24] (a) A. E. Shilov, G. B. Shulpin, Chem. Rev. 97 (1997) 2879; (b) G. B. Shulpin, G. V. Nizova, A. T. Nikitaev, J. Organomet. Chem. 276 (1984) 115; (c) C. Crocker, R. J.

Errington, R. Markham, C. J. Moulton, B. L. Shaw, J. Chem. Soc., Dalton.Trans. (1982) 387.
[25] (a) M. Ramesh, M. Kalidass, M. Jaccob, D. Kaleeswaran, G. Venkatachalam, J. Organomet. Chem. 830 (2017) 33;
(b) S. Baksi, R. Acharyya, F. Basuli, S.M. Peng, G.H. Lee, M. Nethaji, S. Bhattacharya, Organometallics 26 (2007) 6596.
[26] J. Xiang, L.T.-L. Lo, C.-F. Leung, S.-M. Yiu, C.-C. Ko, T.-C. Lau, Organometallics 31 (2012) 7101.
[27] (a) K. Ghosh, R. Kumar, K. Kumar, A. Ratnam, U.P. Singh, RSC Adv. 4 (2014) 43599;
(b) R. Acharyya, S.M. Peng, G.H. Lee, S. Bhattacharya, Inorg. Chem. 42 (2003) 7378.
[28] N. Raja, M.U. Raja, R. Ramesh, Inorg. Chem. Commun. 19 (2012) 51–54.
[29] K. ChiChak, U. Jacquenard, N.R. Branda, Eur. J. Inorg. Chem. (2002) 357.
[30] K.N. Kumar, R. Ramesh, Y. Liu, J. Mol. Catal. A Chem. 265 (2007) 218.
[31] G.K. Lahiri, S. Bhattacharya, M. Mukherjee, A.K. Mukherjee, A. Chakravorty, Inorg. Chem. 26 (1987) 3359.
[32] P.K. Sinha, J. Chakravarty, S. Bhattacharya, Polyhedron 16 (1997) 81.
[33] V. Arun, N. Sridevi, P.P. Robinson, S. Manju, K.K.M. Yusuff, J. Mol. Catal. A: Chem. 304 (2009) 191.
[34] R.N. Prabhu, D. Pandiarajan, R. Ramesh, J. Organomet. Chem. 694 (2009) 4170.
[35] N. Chitrapriya, V. Mahalingam, L.C. Channels, M. Zeller, F.R. Fronczek, K. Natarajan, Inorg. Chim. Acta. 361 (2008) 2841.
[36] S. Pal, S. Pal, Eur. J. Inorg. Chem. (2003) 4244.
[37] A. Shyamala, A.R. Chakravarthy, Polyhedron 12 (1993) 1545.
[38] A. Basu, T.G. Kasan, N.Y. Sapre, Inorg. Chem. 27 (1988) 4539.
[39] A.M. El-Hendawy, A.E. Kourashy, M.M. Shanab, Polyhedron 11 (1992) 523.
[40] D. Chattergee, A. Mitra, B.C. Roy, J. Mol. Catal. A. Chem. 161 (2000) 17.
[41] M.S. El-Shahawi, A.F. Shoair, Spectrochim. Acta A. 60 (2004) 121.
[42] Y. Tsuji, T. Ohta, T.T. Ido, H. Minbu, Y. Watanabe, J. Organomet. Chem. 270 (1984) 333.
[43] N. Ahmed, J.J. Levison, S.D. Robinson, M.F. Uttley, Inorg. Synth. 15 (1974) 45.
[44] R.A. Sanchez-Delgado, W.Y. Lee, S.R. Choi, Y. Cho, M. Jun, J. Trans. Met. Chem. 16 (1991) 241.
[45] R. Nandhini, M. Ramesh, G. Prabusankar, G. Venkatachalam, Inorg. Chem. Commun. 85 (2017) 84–88.
[46] G.M. Sheldrick, Acta Cryst., A. 64 (2008) 112.
[47] L.J. Farrugia, J. Appl. Cryst. 30 (1997) 565.
[48] M.J. Frisch, G.W. Trucks, H.B. Schlegel, G.E. Scuseria, M.A. Robb, J.R. Cheeseman, G. Scalmani, V. Barone, B. Mennucci, G.A. Petersson, H. Nakatsuji, M. Caricato, X. Li, H.P. Hratchian, A.F. Izmaylov, J. Bloino, G. Zheng, J.L. Sonnenberg, M. Hada, M. Ehara, K. Toyota, R. Fukuda, J. Hasegawa, M. Ishida, T. Nakajima, Y. Honda, O. Kitao, H. Nakai, T. Vreven, J.A. Montgomery Jr., J.E. Peralta, F. Ogliaro, M. Bearpark, J.J. Heyd, E. Brothers, K.N. Kudin, V.N. Staroverov, R. Kobayashi, J. Normand, K. Raghavachari, A. Rendell, J.C. Burant, S.S. Iyengar, J. Tomasi, M. Cossi, N. Rega, J.M. Millam, M. Klene, J.E. Knox, J.B. Cross, V. Bakken, C. Adamo, J. Jaramillo, R. Gomperts, R.E. Stratmann, O. Yazyev, A.J. Austin, R. Cammi, C. Pomelli, J. Ochterski, R.L. Martin, K. Morokuma, V.G. Zakrzewski, G.A. Voth, P. Salvador, J.J. Dannenberg, S. Dapprich, A.D. Daniels, O. Farkas, J.B. Foresman, J. V. Ortiz, J. Cioslowski, D.J. Fox, GAUSSIAN 09, (Revision D01), Gaussian Inc, Wallingford, CT, 2009.
[49] C. Lee, W. Yang, R.G. Parr, Phys. Rev. 37 (1988) 785.
[50] D. Becke, J. Chem. Phys. 98 (1993) 5648.
[51] P.J. Hay, W.R. Wadt, J. Chem. Phys. 82 (1985) 299.
[52] W.R. Wadt, P.J. Hay, J. Chem. Phys. 82 (1985) 284.
[53] M. Jaccob, A. Ansari, B. Bhandey, G. Rajaraman, Dalton Trans. 42 (2013) 16518.
[54] M. Jaccob, G. Rajaraman, Dalton Trans. 41 (2012) 10430.